

Supplementary Information

Facile and elegant self-organization of Ag nanoparticles and TiO₂ nanorods on V₂O₅ nanosheets as a superior cathode material of lithium-ion batteries

Du-Juan Yan,^cXiao-Dong Zhu,^{a,b,*}Ke-Xin Wang,^cXiao-Tian Gao,^cYu-Jie Feng,^aKe-Ning Sun^{a,b,*} and Yi-Tao Liu^{d,*}

^aState Key Laboratory of Urban Water Resource and Environment, Harbin Institute of Technology,

Harbin 150090, China.

^bAcademy of Fundamental and Interdisciplinary Sciences, Harbin Institute of Technology,

Harbin 150080, China.

^cDepartment of Chemistry, Harbin Institute of Technology, Harbin 150001, China.

^dState Key Laboratory of Precision Measurement Technology and Instruments,

Department of Precision Instrument, Tsinghua University, Beijing 100084, China.

*Corresponding Authors.

E-mail addresses: zxd9863@163.com, keningsunhit@126.com, liu-xt03@mails.tsinghua.edu.cn.

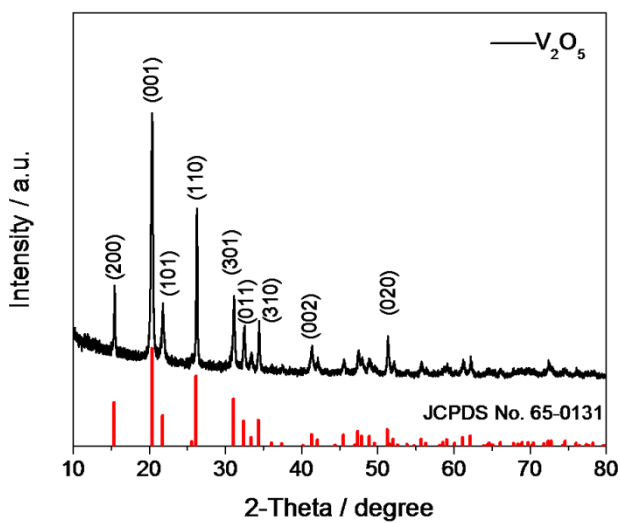


Fig. S1—XRD pattern of V_2O_5 nanosheets.

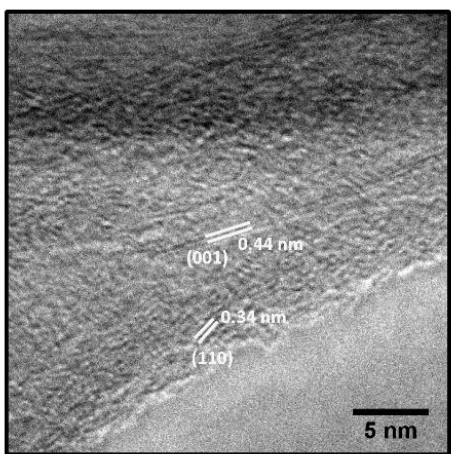


Fig. S2– HRTEM image of V₂O₅ nanosheets revealing lattice fringe distances of 0.44 and 0.34 nm corresponding to the (001) and (110) planes of V₂O₅ (*Nano Lett.*, 2010, **10**, 4750; *Small*, 2014, **10**, 3032; *Nanoscale*, 2013, **5**, 556).

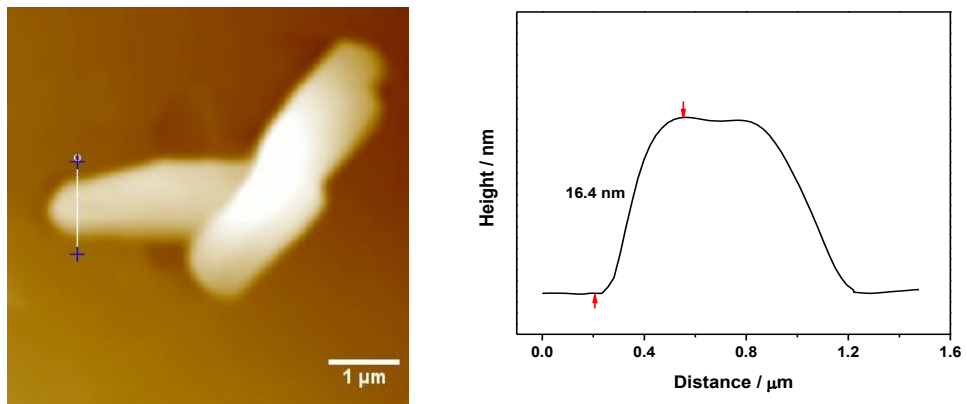


Fig. S3– AFM image of V₂O₅ nanosheets and the corresponding height profile. This image reveals V₂O₅ nanosheets with a lateral size on the micrometer scale and a thickness of 16.4 nm, corresponding to an aspect ratio of ~200. This morphology (with relatively smooth surfaces) is in good agreement with what is observed under TEM and SEM, confirming the successful exfoliation of V₂O₅ nanosheets.

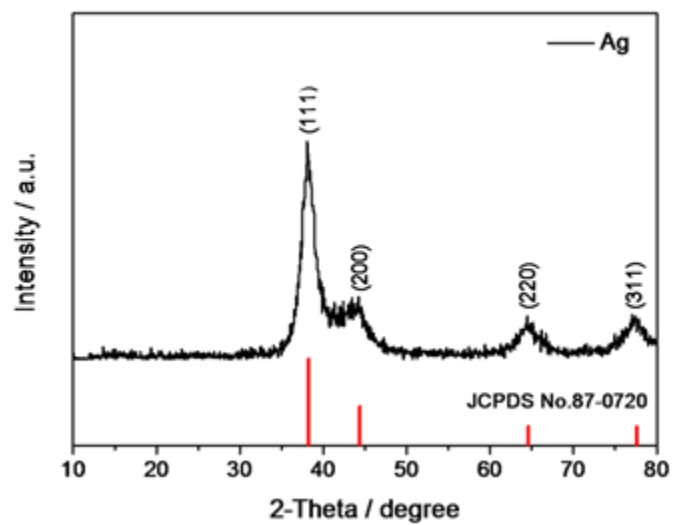


Fig. S4—XRD pattern of Ag nanoparticles.

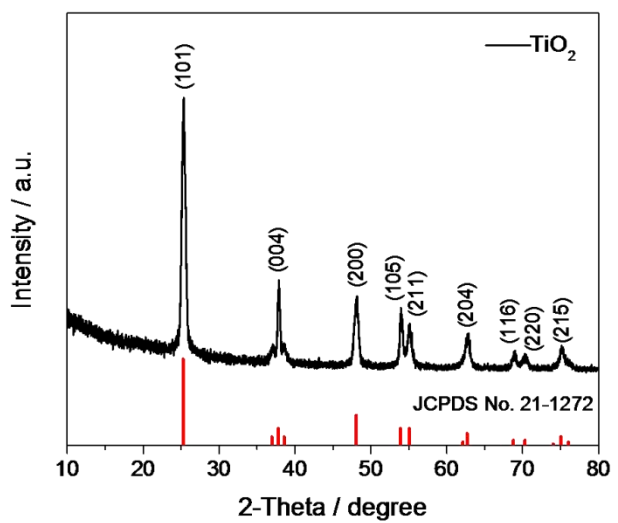


Fig. S5—XRD pattern of TiO_2 nanorods.

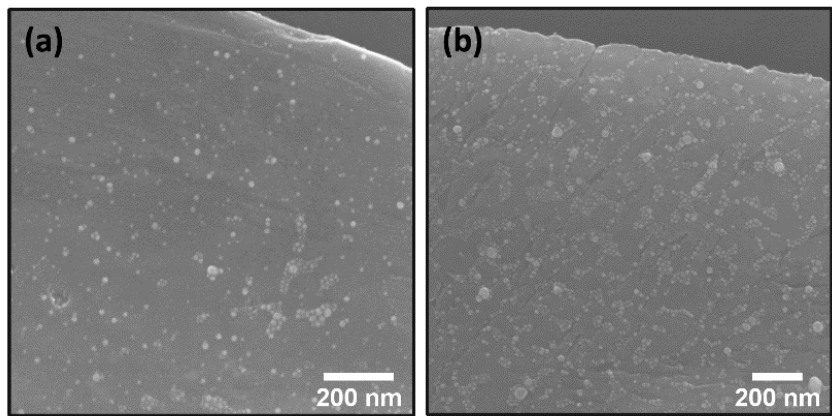


Fig. S6– SEM images of Ag/V₂O₅ hybrid architectures at weight ratios of (a) 10 : 100 and (b) 20 : 100.

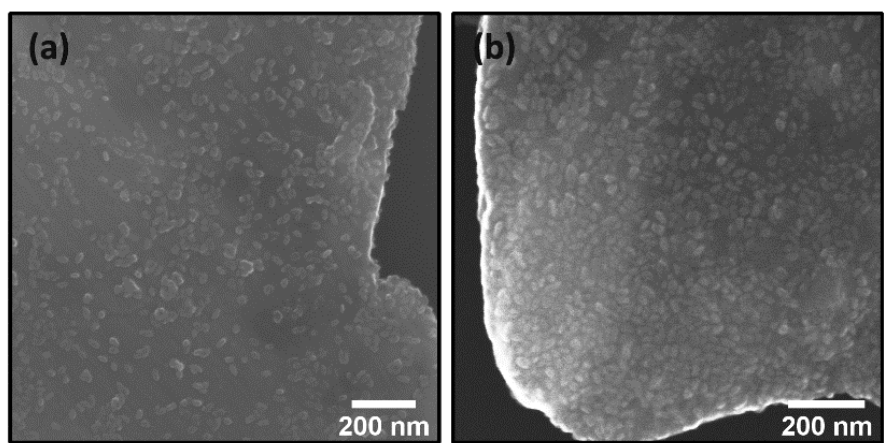


Fig. S7– SEM images of $\text{TiO}_2/\text{V}_2\text{O}_5$ hybrid architectures at weight ratios of (a) 10 : 100 and (b) 20 : 100.

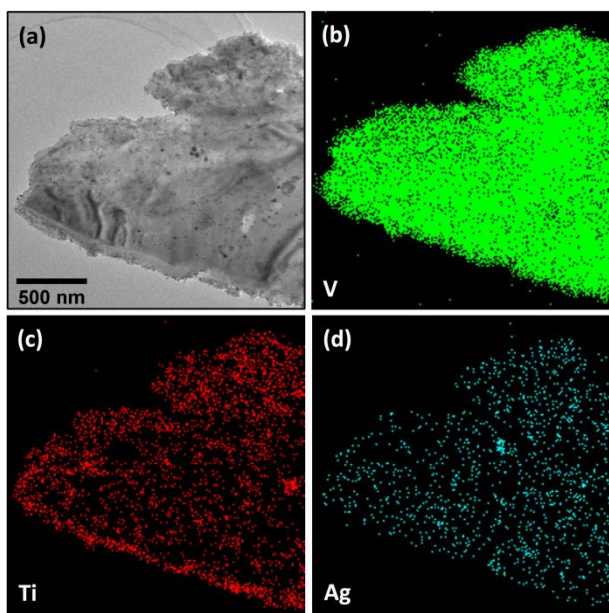


Fig. S8– (a) TEM image of Ag–TiO₂/V₂O₅ hybrid architectures and corresponding EDS maps of elemental (b) V, (c) Ti and (d) Ag.

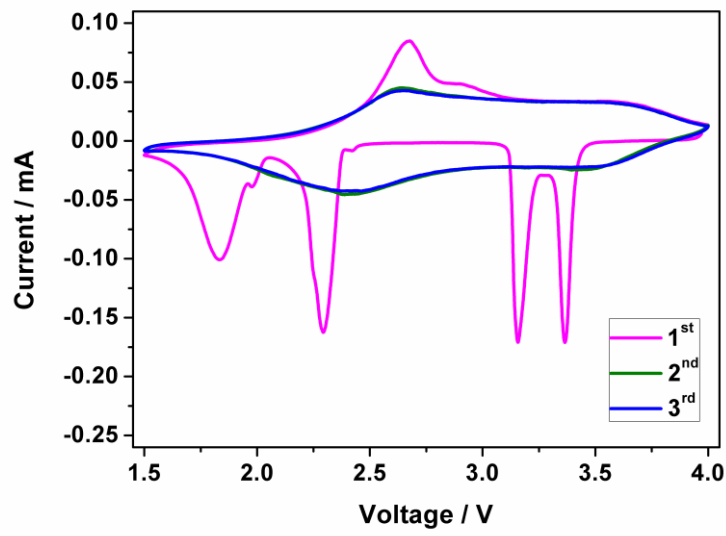


Fig. S9– Initial three CV curves of neat V_2O_5 nanosheets.

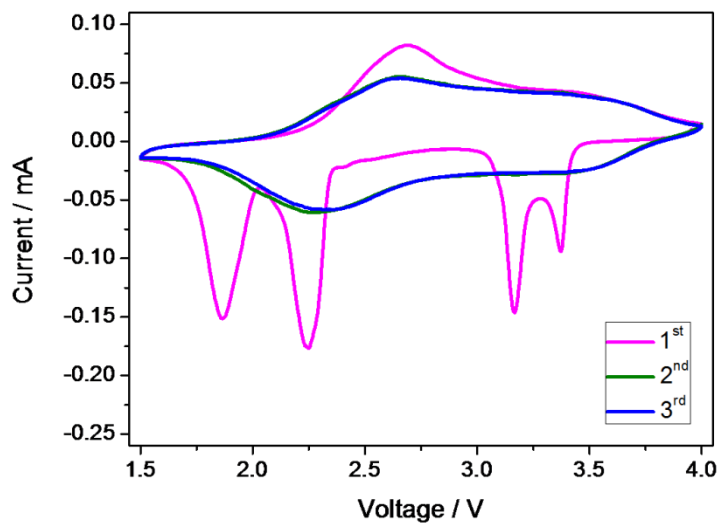


Fig. S10– Initial three CV curves of Ag/V₂O₅ hybrid architectures.

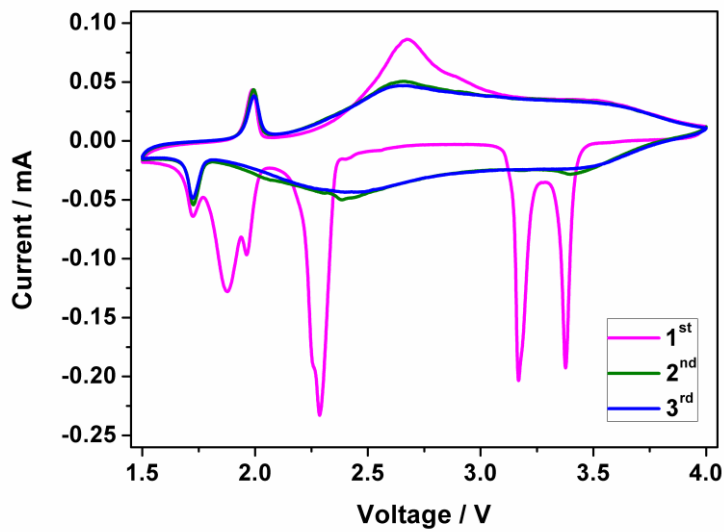


Fig. S11– Initial three CV curves of $\text{TiO}_2/\text{V}_2\text{O}_5$ hybrid architectures.

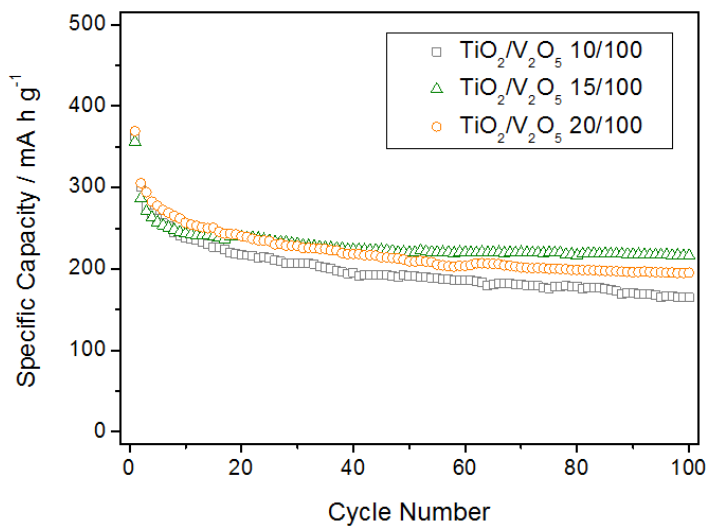


Fig. S12– Cycle behaviours of $\text{TiO}_2/\text{V}_2\text{O}_5$ hybrid architectures (10/100,15/100 and 20/100) at a current density of 100 mA g^{-1} .

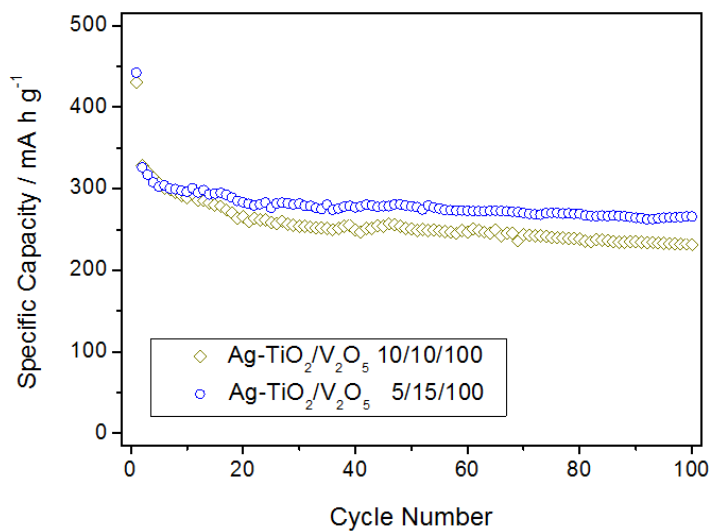


Fig. S13– Cycle behaviours of Ag–TiO₂/V₂O₅ hybrid architectures (5/15/100 and 10/10/100) at a current density of 100 mA g^{−1}.

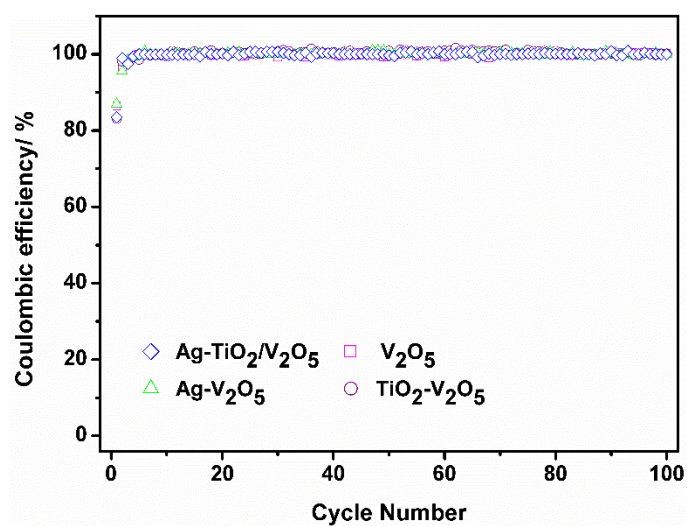


Fig.S14– Coulombic efficiencies of Ag/V₂O₅, TiO₂/V₂O₅ and Ag–TiO₂/V₂O₅ hybrid architectures as well as neat V₂O₅ nanosheets.

Table S1. Elemental composition of Ag/V₂O₅ (5/100), TiO₂/V₂O₅ (15/100) and Ag–TiO₂/V₂O₅ (5/15/100) hybrid architectures.

	Ag (wt%)	Ti (wt%)	V (wt%)	Octadecylamine- coated Ag (wt%)	Oleylamine-coat ed TiO ₂ (wt%)	V ₂ O ₅ (wt%)	Samples
Actual ratio	4.26	—	53.25	4.81	—	95.01	Ag/V ₂ O ₅
Starting ratio	—	—	—	4.76	—	95.24	(5/100)
Actual ratio	—	6.22	48.32	—	12.50	86.22	TiO ₂ /V ₂ O ₅
Starting ratio	—	—	—	—	13.04	86.96	(15/100)
Actual ratio	3.67	6.08	46.88	4.15	12.21	83.65	Ag–TiO ₂ /V ₂ O ₅
Starting ratio	—	—	—	4.17	12.50	83.33	(5/15/100)